Since January 2020 Elsevier has created a COVID-19 resource centre with free information in English and Mandarin on the novel coronavirus COVID-19. The COVID-19 resource centre is hosted on Elsevier Connect, the company's public news and information website.

Cytotherapy 22 (2020) 458–472

Contents lists available at ScienceDirect

CYTOTHERAPY

journal homepage: www.isct-cytotherapy.org

FULL-LENGTH ARTICLE

Manufacturing

Nanofiltration of growth media supplemented with human platelet lysates for pathogen-safe xeno-free expansion of mesenchymal stromal cells

Lassina Barro[a], Ouada Nebie[b], Ming-Sheng Chen[b], Yu-Wen Wu[b], Mickey BC Koh[c,d], Folke Knutson[e], Naoto Watanabe[f], Masayasu Takahara[f], Thierry Burnouf[a,b,g,*]

[a] International PhD Program in Biomedical Engineering, College of Biomedical Engineering, Taipei Medical University, Taipei, Taiwan
[b] Graduate Institute of Biomedical Materials and Tissue Engineering, College of Biomedical Engineering, Taipei Medical University, Taipei, Taiwan
[c] Department of Haematology, St George's University Hospitals Foundation NHS Trust, London, UK
[d] Blood Sciences Group, Health Sciences Authority, Singapore
[e] Clinical Immunology and Transfusion Medicine IGP, Uppsala University, Uppsala, Sweden
[f] Asahi Kasei Medical Co., Ltd., Tokyo, Japan
[g] International Program in Cell Therapy and Regeneration Medicine, Taipei Medical University, Taipei, Taiwan

ARTICLE INFO

Article History:
Received 11 January 2020
Accepted 22 April 2020

Key Words:
HPL
human platelet lysates
mesenchymal stromal cells
nanofiltration
prion
virus

ABSTRACT

Background aims: Human platelet lysate can replace fetal bovine serum (FBS) for xeno-free *ex vivo* expansion of mesenchymal stromal cells (MSCs), but pooling of platelet concentrates (PCs) increases risks of pathogen transmission. We evaluated the feasibility of performing nanofiltration of platelet lysates and determined the impact on expansion of bone marrow–derived MSCs.
Methods: Platelet lysates were prepared by freeze-thawing of pathogen-reduced (Intercept) PCs suspended in 65% storage solution (SPP+) and 35% plasma, and by serum-conversion of PCs suspended in 100% plasma. Lysates were added to the MSC growth media at 10% (v/v), filtered and subjected to cascade nanofiltration on 35- and 19-nm Planova filters. Media supplemented with 10% starting platelet lysates or FBS were used as the controls. Impacts of nanofiltration on the growth media composition, removal of platelet extracellular vesicles (PEVs) and MSC expansion were evaluated.
Results: Nanofiltration did not detrimentally affect contents of total protein and growth factors or the biochemical composition. The clearance factor of PEVs was >3 log values. Expansion, proliferation, membrane markers, differentiation potential and immunosuppressive properties of cells in nanofiltered media were consistently better than those expanded in FBS-supplemented media. Compared with FBS, chondrogenesis and osteogenesis genes were expressed more in nanofiltered media, and there were fewer senescent cells over six passages.
Conclusions: Nanofiltration of growth media supplemented with two types of platelet lysates, including one prepared from pathogen-reduced PCs, is technically feasible. These data support the possibility of developing pathogen-reduced xeno-free growth media for clinical-grade propagation of human cells.

Introduction

It is now well established that human platelet lysate (HPL) made from clinical-grade platelet concentrates (PCs) can be used as a xeno-free supplement for propagating human cells, including mesenchymal stromal cells (MSCs), for therapeutic applications. The advantages of HPL include its human origin, which eliminates the immunological and infectious risks possibly associated with the clinical use of animal sera [1–5]. In addition, the production of PCs, as performed in blood establishments, is under the supervision of regulatory authorities and thus, meets good manufacturing practice requirements in all advanced economies [4,5]. The availability of HPL as an alternative supplement for MSCs *in vitro* expansion, when chemically defined media are not available, is also important considering the expected growth in needs of the regenerative medicine and cell therapy industries [6]. The industrial feasibility of using platelet lysates for clinical-grade expansion of therapeutic human cells is further supported by recent studies which

* Correspondence: Thierry Burnouf, Ph.D., Graduate Institute of Biomedical Materials and Tissue Engineering, College of Biomedical Engineering, Taipei Medical University, 250 Wu-Xing Street, Taipei 11031, Taiwan.
E-mail address: thburnouf@gmail.com (T. Burnouf).

https://doi.org/10.1016/j.jcyt.2020.04.099
1465-3249/

demonstrated that "outdated" PCs, no longer suitable for transfusion, can serve as a suitable source for lysate production, thereby increasing the potential supply [7,8].

Ensuring the consistency in quality and safety of platelet lysates is important [4,5,9,10]. Consistency in quality and performance requires the pooling of a sufficient number of PC donations to counterbalance variability among donors [1,2,11,12]. Pooling, however, increases the risk of contamination by bloodborne pathogens, notably viruses, despite donor screening and donation testing for infectious agents because the sensitivity and selectivity of these two measures have limits [5]. Particular concerns exist with regard to untested emerging viruses, such as West Nile virus, Dengue virus, Zika virus, or coronaviruses, such as severe acute respiratory syndrome coronavirus (SARS-CoV)-1 or -2 if they are present in an infectious form in the blood of asymptomatic donors [13–17]. The ultimate approach to ensure the pathogen safety of pooled lysates, as for any pooled blood products, is by implementing one or two robust and complementary pathogen inactivation or removal treatments [18,19]. Among those, one robust pathogen removal technology is nanofiltration, a step of filtration using membranes of a few nanometers capable of removing viruses, and possibly other pathogens like prions, based on size-exclusion [20,21].

In this study, for the first time, we evaluated the possibility of nanofiltering growth media supplemented with two types of platelet lysates obtained from expired human PCs subjected to psoralen/UVA (Intercept) treatment or left untreated. We also assessed the capacity of using such nanofiltered growth media to expand bone marrow (BM)-MSCs. Finally, we monitored the impacts of nanofiltration on platelet extracellular vesicles (PEVs) present in platelet lysate-supplemented media.

Methods

The overall study design is shown in Figure 1.

Source of PCs

The sources of PCs have been described previously [22]. Briefly, five apheresis PC donations were collected using the Trima Accel platelet collection system (TerumoBCT, Lakewood, CO, USA) at the Uppsala University Blood Bank (Uppsala, Sweden) from volunteer donors. The donations were leukoreduced, resuspended in a 65% platelet additive solution (SSP) and 35% plasma, and pathogen-reduced using the Intercept blood system (psoralen/UVA; Cerus Corp., Concord, CA) [23]. After 7 days of storage (to reach the expiry date), the PCs were frozen at −40°C. In addition, six apheresis PC donations (MCS+ Mobile Collection System—Haemonetics, Braintree, MA, USA) suspended in 100% plasma were obtained from the Taipei Blood Center (Guandu, Taipei, Taiwan) after 5 days of storage (to reach the expiry date). All collections were performed following the validated standard operating procedures in place in these two licensed blood establishments and following the recommendations of the suppliers of the apheresis equipment.

Preparation of the platelet lysates

To prepare Intercept pathogen-reduced (I)- I-HPL (Figure 1), Intercept-treated PC units were thawed (Taipei Medical University, Taipei, Taiwan) in their storage bags at 35 ± 1°C for approximately 30 min, pooled to obtain a total volume of approximately 1 L, and subjected to two additional freeze/thaw cycles (−80/+35°C) [22,24,25]. I-HPL were then centrifuged (at 6000*g* for 30 min at 22 ± 1°C) to pelletize

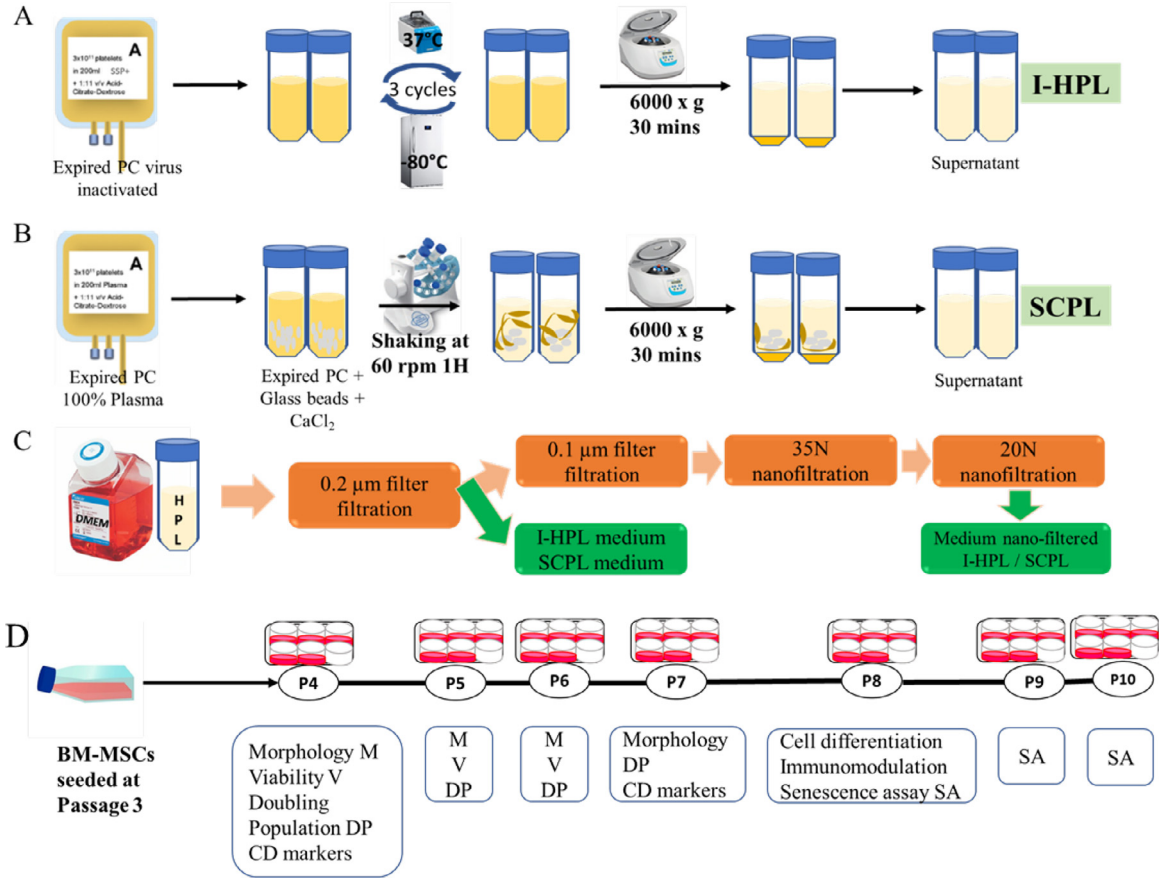

Figure 1. Materials and methods. (A) I-HPL preparation process. (B) SCPL preparation process. (C) Cell culture medium preparation process. (D) BM-MSC culture process with different assessments applied. (Color version of figure is available online).

Table 1
Characteristics of experimental human platelet lysate medium.

	% of Plasma in Raw PC	Raw PC Intercept treated	0.2-μm filtration	0.1-μm filtration	35N nanofiltration	20N nanofiltration	No. of virus inactivation and/or removal steps
SCPL	100	No	Yes	No	No	No	0
mNF-SCPL	100	No	Yes	Yes	Yes	Yes	1
I-HPL	35	Yes	Yes	No	No	No	1
mNF-IHPL	35	Yes	Yes	Yes	Yes	Yes	2

the cell debris. The supernatant was recovered, aliquoted (10 mL), and stored at −20°C until use.

To prepare the serum-converted HPL (SCPL), pooled standard PCs formulated in 100% plasma were activated by calcium chloride (at a final concentration of 23 mmol/L with glass beads) [24]. The mixture was shaken for 1 h at 25 ± 1°C to activate the coagulation cascade, degranulate the platelets, release growth factors, and convert fibrinogen into fibrin. The fibrin clot attached to the glass beads was readily removed, and the suspension was centrifuged, aliquoted and frozen as described in the preceding text.

Media nanofiltration processes

Dulbecco's modified Eagle's medium (DMEM)/high-glucose medium supplemented with 1% GlutaMax 100 × (Gibco, Life Technologies, Grand Island, NY), and 1% penicillin-streptomycin (Gibco, Life Technologies) was mixed with 10% (v/v) I-HPL (2 U/mL heparin added) or SCPL. The mixture was processed as described in Figure 1C and Table 1. Briefly, the mixture was filtered on 0.22-μm PN 4612 and 0.1-μm PN 4611 filters (Pall Life Science, Ann Arbor, MI, USA), then 400 mL was nanofiltered through 0.01-m^2 Planova 35N 35NZ-010 at a flow rate of 1 mL/min, and then through 0.01-m^2 Planova 20N 20NZ-010 filters at a flow rate of 0.8 mL/min (Asahi Kasei Medical, Tokyo, Japan) with monitoring of the protein adsorption at 280 nm, and pressure by an AKTA chromatographic system (GE Healthcare Life Sciences, Freiburg, Germany). The nanofilters were connected to the AKTA system and placed into a Super-CO 150 oven (Enshine Scientific, Taipei, Taiwan) with the temperature maintained at 37°C during the process (supplementary Figure 1). The nanofiltered flow-medium (mNF) was aliquoted and stored at −20°C until use. The starting I-HPL and SCPL were used as controls to specifically detect the impacts of the nanofiltration process on the protein composition, chemical composition, capacity to expand BM-MSCs, and removal of PEVs.

Analysis of particles and trophic factors in the filtered medium

Samples were detected by dynamic light scattering (DLS) to determine the population size and by a nanoparticle tracking analysis (NTA) to determine the size and concentration of EVs. The protein content was measured using a bicinchoninic acid (BCA) protein assay kit (Pierce Biotechnology, Rockford, IL, USA). Brain-derived neurotrophic factor (BDNF), epidermal growth factor (EGF), fibroblast growth factor (FGF), hepatocyte growth factor (HGF), insulin-like growth factor (IGF), platelet-derived growth factor (PDGF)-AB, transforming growth factor (TGF)-β, vascular endothelial growth factor (VEGF), and platelet factor 4 (PF4) were quantified by a sandwich enzyme-linked immunosorbent assay (ELISA) technique (DuoSet ELISA; R&D Systems, Minneapolis, MN, USA) as previously described [22,24], following the manufacturer's protocol.

Human BM-MSC culture

We seeded BM-MSCs (American Type Culture Collection, Manassas, VA) in 55-cm^2 dishes and cultured them in the earlier-described DMEM containing 10% FBS at 37°C with a 5% CO_2 humidified atmosphere at passage 3. The starting human platelet lysates, I-HPL and SCPLs, and the corresponding nanofiltered media were used for different assessments from passage 4 to passage 10, at a normalized concentration of platelet lysates of 10% (v/v). The growth medium was renewed every 2–3 days.

Population doubling

We measured the population doubling (PD) of BM-MSCs over four passages (Ps). Cells were seeded at 5 × 10^3 cells/cm^2 in six-well plates with various prepared media. After reaching 80%–90% confluence, cells were detached with 0.05% trypsin-EDTA (Sigma, St. Louis, MO, USA) and harvested for counting. Ten microliters of the cells suspension were loaded in the well of the hemocytometer. The cells in the four sets of 16 squares were counted and then divided by 4 squares to get the mean. The mean was multiplied by 10^4 as a concentration of cells in 1 mL. This concentration was multiplied by the total volume of cells harvested from the well to get the total number of cell (Nf). PD was assessed at the end of each P using the following formula: PD = (log10(Nf) − log10(Ni))/log10(2), where Nf denotes the number of cells retrieved at the end of the P, and Ni is the number of cells seeded at the beginning of the P. To calculate the cumulative PD, the number of PDs at the end of each P was added to the PD of the previous P.

Cell viability

Cell viability was evaluated from P4 to P6. We seeded cells (3000 cells/well) in 96-well plates in DMEM supplemented with 10% FBS or in different human platelet lysates conditions. Viability was assessed after 24 and 72 h using CCK-8 (Sigma). The optical density was measured by a TECAN Sunrise ELISA reader (TECAN, MaÈnnedorf, Switzerland) at 450 nm, and viability was expressed as a percent of FBS.

Flow cytometry

We performed a flow cytometric analysis using a Sony SA3800 Spectral Analyzer (Sony Biotechnology, Tokyo, Japan). The following cell surface markers (cluster of differentiation (CD) markers) were analyzed at P1 and P4: CD31 (FITC; BD Bioscience, San Jose, CA, USA), CD45 (FITC; BD Bioscience), CD73 (APC, clone AD2; BD Bioscience), CD90 (PE; BD Bioscience), CD105 (APC, clone 266; BD Bioscience), and human leukocyte antigen (HLA) DR (APC, clone G46-6; BD Bioscience). Adherent cells were harvested after trypsinization. Cells were washed with phosphate-buffered saline (PBS) and incubated at room temperature for 15 min with different anti-human mouse antibodies, and then incubated on ice for 30 min. Four percent paraformaldehyde (PFA) in phosphate buffer was used to fix cells after incubation under previously defined conditions. PFA was discarded after centrifugation (300*g* for 5 min), and cells were re-suspended in PBS for the flow cytometric analysis.

Human BM-MSC differentiation

After four Ps in different experimental media, we assessed the differentiation potential of expanded MSCs at P8 into adipogenic, osteogenic, or chondrogenic lineages as described before [22]. To evaluate

adipogenesis, BM-MSC cells were seeded at a density of 60 000 cells per well in six wells/plate. Adipogenesis was induced by adding 0.5 mmol/L isobutylmethylxantine (IBMX), 1 μmol/L dexamethasone, 10 μmol/L insulin, and 200 μmol/L indomethacin (final concentrations), all from Sigma, to the culture medium. The medium was refreshed every 3 days. The lipid vacuole formation was observed on day 14 using Oil Red O staining. Osteogenesis and chondrogenesis differentiation were evaluated on day 21 by Alizarin Red staining for calcium deposition and by Safranin O staining for glycosaminoglycan (GAG) extracellular matrix (ECM) formation. The cells were seeded at the density of 100 000 cells per well in six wells/plate. Osteogenesis was induced by adding 0.1 μmol/L dexamethasone, 50 μmol/L ascorbic-2-phosphate, and 10 mmol/L B-glycerophosphate (final concentrations). The medium was refreshed every 3 days. Chondrogenesis was induced by adding 250 ng/mL insulin, 10 ng/mL transforming growth factor-beta (TGF-beta) and 50 nmol/L ascorbate-2-phosphate (final concentrations) to the culture media.

Genes expression profiling during BM-MSC differentiation

Samples were collected at day zero of differentiation induction (d0), d7, d10, d14 and d21 to check expressions of genes involved in differentiation: *PPARG* and *ADIPOQ* genes for adipogenesis; *SOX9* and *RUNX2* genes for chondrogenesis; and *SPP1* and *RUNX2* genes for osteogenesis. Total RNA was extracted using a RNeasy Micro Kit (Qiagen, Valencia, CA, USA). Complementary (c)DNA synthesis was performed using 1 μg of total RNA, random primers, and the Superscript III reverse transcriptase (Invitrogen, Carlsbad, CA, USA) at 42°C for 50 min in a final volume of 20 μL. Polymerase chain reaction (PCR) amplification was performed using QuantiTect SYBR Green PCR Mix (Qiagen). Primer sequences, annealing temperatures, and PCR cycling conditions are described in Table 2. β-2M mRNA was used as an internal control. The -$\Delta\Delta$Ct (threshold cycle) was defined as -$\Delta\Delta$Ct = –[(CtGI - CtIC) differentiation sample] – [(CtGI - CtIC) control sample], where GI represents the gene of interest and IC indicates β-2M. The Ct value of cells in the control group at day zero was used as the calibrator. A real-time quantitative (q)PCR analysis of three independent cultures was run for all experiments.

EV recovery from BM-MSC culture

At P7, we seeded cells at 5×10^3 cells/cm^2 in six-well plates in the various media prepared. Media were refreshed after 48 h. Cells were maintained for 3 days of culture, then the medium was collected and centrifuged (6000*g* for 10 min), and the supernatant was retained for an EV analysis and for immunosuppression assessment.

Immunomodulation experiment

We isolated peripheral blood mononuclear cells (PBMCs) from whole blood collected from four healthy donors. PBMCs were stimulated with mitogen phytohemagglutinin (PHA) (Gibco Life Technologies) in different culture media (RPMI-1640 supplemented with 10% FBS or HPL fractions) for 4 days at 37°C with a 5% CO_2 humidified atmosphere. Viability was assessed using CCK-8 for PBMCs cultured alone or PBMCs in medium from BM-MSC culture mixed v/v with new medium, or co-cultured with BM-MSCs, using a 10:1 ratio of PBMCs to BM-MSCs, for 3 days. The percent proliferation inhibition of BM-MSCs was calculated from this formula: I = (1 - (Optic density (OD)pbmc)/ODcc) × 100 (CC, PBMC culture with BM-MSCs). Different culture conditions media were collected and used for interleukin (IL)-6, IL-10 and tumor necrosis factor (TNF) assessments by ELISA methods.

Senescence assay

We performed a senescence assay with BM-MSCs cultured as cells counted from P8 to P10. After reaching 80%–90% confluence, cells were trypsinized and harvested for counting. A second six-well plate was used for histochemical staining of senescent cells. After washing with PBS, cells were fixed and stained using an X-gal solution [26]. The six-well plates were next incubated overnight at 37°C without CO_2. The blue dye formed by senescence-associated β-galactosidase (β-gal) cells was observed under an optical microscope (DMI8 microscope, Leica Wetzlar, Germany), and images were captured. Ten random fields, each from three BM-MSC culture conditions and control cultures, were used to calculate the senescence ratio.

Statistical analysis

All data were from three independent experiments and are presented as the mean ± SD. Statistical analyses were performed using GraphPad Prism software vers. 6.0 (GraphPad Software, La Jolla, CA). An analysis of variance (ANOVA) and *t*-test were used for comparison, and differences were considered significant at $P < 0.05$.

Results

Source materials and nanofiltration

Intercept-treated apheresis PC donations were 180 mL to 220 mL and had a mean platelet count of $3 \times 10^{11} \pm 0.26$ platelets/unit. Standard apheresis PC were 230 to 260 mL and with a platelet count of $5.3 \times 10^{11} \pm 1.2$ platelets/unit. The PCs were used to prepare I-HPL and SCPL and added at a final concentration of 10% (v/v) to the growth media.

Approximately 450 and 350 mL of mNF-IHPL and mNF-SCPL could be nanofiltered within 7 and 6 h at a constant flow-rate of 1 mL/min, respectively, through 0.01 m^2 Planova 35N until the pressure reaches the maximum of 0.1mPa. Approximately 420 and 315 mL of these respective Planova 35N-nanofiltered solutions could pass through 0.01 m^2 Planova 20N within 8 h at constant 0.8 mL/min without reaching the maximum pressure of 0.1 mPa (supplementary Figure 2).

Chemical composition of growth media

The chemical compositions of different media are summarized in Table 3. The mNF-IHPL and mNF-SCPL had significantly lower levels of ferritin (3 ± 1 and 4.33 ± 1.15 ng/mL, respectively), calcium (Ca)

Table 2
Primer sequences used for qPCR analysis.

Gene	Accession	Forward Primers (5′→3′)	Reverse Primers (5′→3′)	Annealing Temp (°C)	Product Size (bp)
ADIPOQ	NM_004797.3	GATGAAGTCCTGTCTTGGAAGG	CAGCACTTAGAGATGGAGTTGG	63	103
PPARG	NM_138711	GCAGGAGATCTACAAGGACTTG	CCCTCAGAATAGTGCAACTGG	63	85
RUNX2	NM_001015051.3	GGTTAATCTCCGCAGGTCACT	CACTGTGCTGAAGAGGCTGTT	65	122
SOX9	NM_000346.3	AGGTGCTCAAAGGCTACGAC	GTAATCCGGGTGGTCCTTCT	64	104
SPP1	NM_001251830.1	TGGCCGAGGTGATAGTGTGGTTTA	AACGGGGATGGCCTTGTATGC	68	150
β-2M	NM_004048.2	GTCTCGCTCCGTGGCCTTA	TGAATCTTTGGAGTACGCTGGATA	56	81

Table 3
Biochemical content of different experimental medium.

Item analyzed	FBS value	I-HPL value	P	mNF-IHPL value	P	SCPL value	P	mNF-SCPL value	P
Total protein (mg/mL)	4.33 ± 0.58	2.67 ± 0.58	*	2.67 ± 0.58	*	4.67 ± 0.58		4.33 ± 0.58	
Albumin (mg/mL)	3.33 ± 0.58	2.00	*	2.00	*	4.00		3.00	
Fibrinogen (mg/mL)	<0.40	<0.40		<0.40		<0.40		<0.40	
Hemoglobin (g/dL)	<0.10	<0.10		<0.10		<0.10		<0.10	
Ferritin (ng/mL)	1.00	5.33 ± 0.58	****	3 ± 1	*/#	7.67 ± 0.58	****	4.33 ± 1.15	**/+
Glucose AC (mg/dL)	413.67 ± 2.08	391 ± 4	****	396 ± 14		406.67 ± 12.58		408 ± 15.10	
Triglyceride (mg/dL)	9.00	9.00		9.00		9.67 ± 1.15		9.00	
Cholesterol (mg/dL)	4.00	5.00		4.00		10 ± 1	****	4.00	++++
$VitB_{12}$ (pg/mL)	71.60 ± 3.11	50.00	****	50.00	****	54.50 ± 7.79	*	71.63 ± 3.80	
Folate (ng/mL)	>20.00	>20.00		>20.00		>20.00		>20.00	
Na (mEq/L)	155.67 ± 0.58	157.33 ± 1.53		160.33 ± 2.08	*	153.67 ± 1.53		157.33 ± 3.21	
Cl (mEq/L)	126.00	122.67 ± 1.15	**	124.33 ± 1.53		131.33 ± 8.50		134.67 ± 9.61	
Mg (mg/dL)	2.07 ± 0.06	1.93 ± 0.06	*	1.70 ± 0.10	**/#	1.87 ± 0.12	*	1.77 ± 0.21	*
Ca (mg/dL)	7.43 ± 0.06	5.83 ± 0.23	****	3.03 ± 0.32	****/####	15.1 ± 1.15	****	11.67 ± 1.23	**/+
Fe (ug/dL)	22.33 ± 0.58	5.33 ± 0.58	****	5.00	****	7 ± 1	****	6.67 ± 0.58	****
P (mg/dL)	3.23 ± 0.06	6.73 ± 0.15	****	5.43 ± 0.31	****/##	2.03 ± 0.38	**	0.83 ± 0.15	****/++
K (mEq/L)	6.30	5.57 ± 0.06	****	5.67 ± 0.06	****	5.27 ± 0.06	****	5.40 ± 0.10	****
TIBC (ug/dL)	95.67 ± 9.07	81.33 ± 9.61		78.34 ± 6.66		84 ± 5.29		83.33 ± 5.51	
UIBC (ug/dL)	73.33 ± 8.50	77.67 ± 7.02		75 ± 9.54		77 ± 5.20		76.67 ± 5.51	

*FBS vs. HPL; #I-HPL vs. mNF-IHPL; + SCPL vs. mNF-SCPL. *, # or + $P < 0.05$; **, ## or ++ $P < 0.01$; ***, ### or +++ $P < 0.001$; ****, #### or ++++ $P < 0.0001$.

(3.03 ± 0.32 and 11.67 ± 1.23 mg/dL), and phosphorus (5.43 ± 0.31 and 0.83 ± 0.15 mg/dL) compared to I-HPL or SCPL ($P < 0.05$, $P < 0.0001$ or $P < 0.05$ and $P < 0.01$, respectively). Similar significant differences were found for ferritin, magnesium (Mg), Ca, iron (Fe), phosphorus and potassium (K) for I-HPL and SCPL and their derived nanofiltered medium compared with FBS. Total protein and albumin contents were significantly less in I-HPL and mNF-IHPL compared to FBS, SCPL, and mNF-SCPL ($P < 0.05$), as expected.

Contents of growth factors and PF4

Growth factor contents are shown in Figure 2. There were significant decreases in BDNF, EGF, PDGF-AB, TGF-β and VEGF contents in the 10% I-HPL-medium between before and after nanofiltration (from 4284 to 106 pg/mL $P < 0.001$; 414 to 292 pg/mL $P < 0.001$; 8693 to 2845 pg/mL $P < 0.001$; 4465 to 3121 pg/mL $P < 0.05$; and 50 to 38 pg/mL $P < 0.05$, respectively). Similar decreases were found in the 10% SCPL-medium before and after nanofiltration (from 3586 to 911 pg/mL $P < 0.001$; 86 to 48 pg/mL $P < 0.01$; 5544 to 3846 pg/mL $P < 0.001$; 3617 to 2657 pg/mL $P < 0.01$; and 159 to 95 pg/mL $P < 0.05$, respectively). In contrast, no significant difference was found in HGF or IGF contents in I-HPL supplemented media, regardless of whether they were nanofiltered.

PEV removal

Particle sizes and concentrations of PEVs in the various media as determined by DLS and NTA, respectively, are shown in Table 4. Figure 3A and 3B show the size distribution at different preparation steps of the nanofiltered medium. Concentrations of PEVs significantly decreased between the unfiltered and the 20N nanofiltered media (5.12×10^{11} to 4.79×10^{8}, $P < 0.01$ for I-HPL; 9.17×10^{11} to 1.15×10^{9}, $P < 0.001$ for SCPL). Nanofiltration removed mostly PEVs as indicated by the difference between 0.22-μm filtration and 20N nanofiltration (4.65×10^{11} to 4.79×10^{8} $P < 0.01$ for I-HPL and 8.89×10^{11} to 1.15×10^{9} $P < 0.05$ for SCPL).

Impact of nanofiltration on BM-MSC proliferation

The typical morphology of BM-MSCs which expanded from P4 to P7 is shown in Figure 4A. BM-MSCs cultured in all media supplemented by platelet lysates showed a more elongated spindle-shaped morphology compared with those cultured in FBS. Cell growth was accelerated in all platelet lysate media compared with FBS, and the cumulative PDs were 16.57 in SCPL, 12.72 in I-HPL, 12.30 in mNF-SCPL, 10.0 in mNF-IHPL and 9.27 in FBS. However, at P6 and P7, the proliferation time increased. The cumulative PDs in the nanofiltered mNF-IHPL and mNF-SCPL media were significantly higher than that in FBS ($P < 0.0001$). Significant differences ($P < 0.0001$) were found between I-HPL and mNF-I-HPL, and between SCPL and mNF-SCPL media. Cell viabilities analyzed by CCK-8 were similar in mNF-IHPL and FBS-based media. However, MSCs propagated in mNF-IHPL medium had lower viability compared to those in I-HPL medium ($P < 0.001$) at 72 h in P6. Cell viability was significantly higher ($P < 0.0001$) when cells were expanded in other media supplemented with the other platelet lysates at P6 (Figure 4E).

Impacts of nanofiltration on BM-MSC marker expressions

Cell surface markers at P4 are shown in Figure 5A. All cultures expressed the MSC markers of CD73, CD90 and CD105. However, CD105 expression was <95%. TCD105 expression was high (>95%) at P7 as shown in Figures 5B and 5C. CD31 and CD45, primitive hematopoietic progenitors and endothelial cells, were <5% in all media. HLA DR expression was <5% in all media supplemented with human platelet lysates, and slightly higher in FBS medium (8%–9%).

Impacts of nanofiltration on BM-MSC differentiation

The differentiation capacity of BM-MSCs into osteoblasts, chondrocytes and adipocytes was effective under all conditions (Figure 6). Lipid droplet accumulation (adipogenesis) was significantly higher in cells expanded in medium supplemented with FBS compared with I-HPL, mNF-IHPL and mNF-SCPL ($P < 0.05$, $P < 0.0001$ and $P < 0.0001$, respectively). No significant difference was found between SCPL and FBS. Significant differences were found between I-HPL and mNF-IHPL ($P < 0.05$) and between SCPL and mNF-SCPL ($P < 0.001$). ECM formation during chondrogenesis, as assessed by glycosaminoglycan, was significantly higher in all human platelet lysates supplements ($P < 0.01$) compared with FBS supplementation. Calcium deposition, a characteristic of osteogenesis, was significantly higher ($P < 0.0001$) in all platelet lysate-supplemented media than in FBS-supplemented media. Significant differences were found between I-HPL and mNF-IHPL ($P < 0.0001$), and between SCPL and mNF-SCPL ($P < 0.0001$).

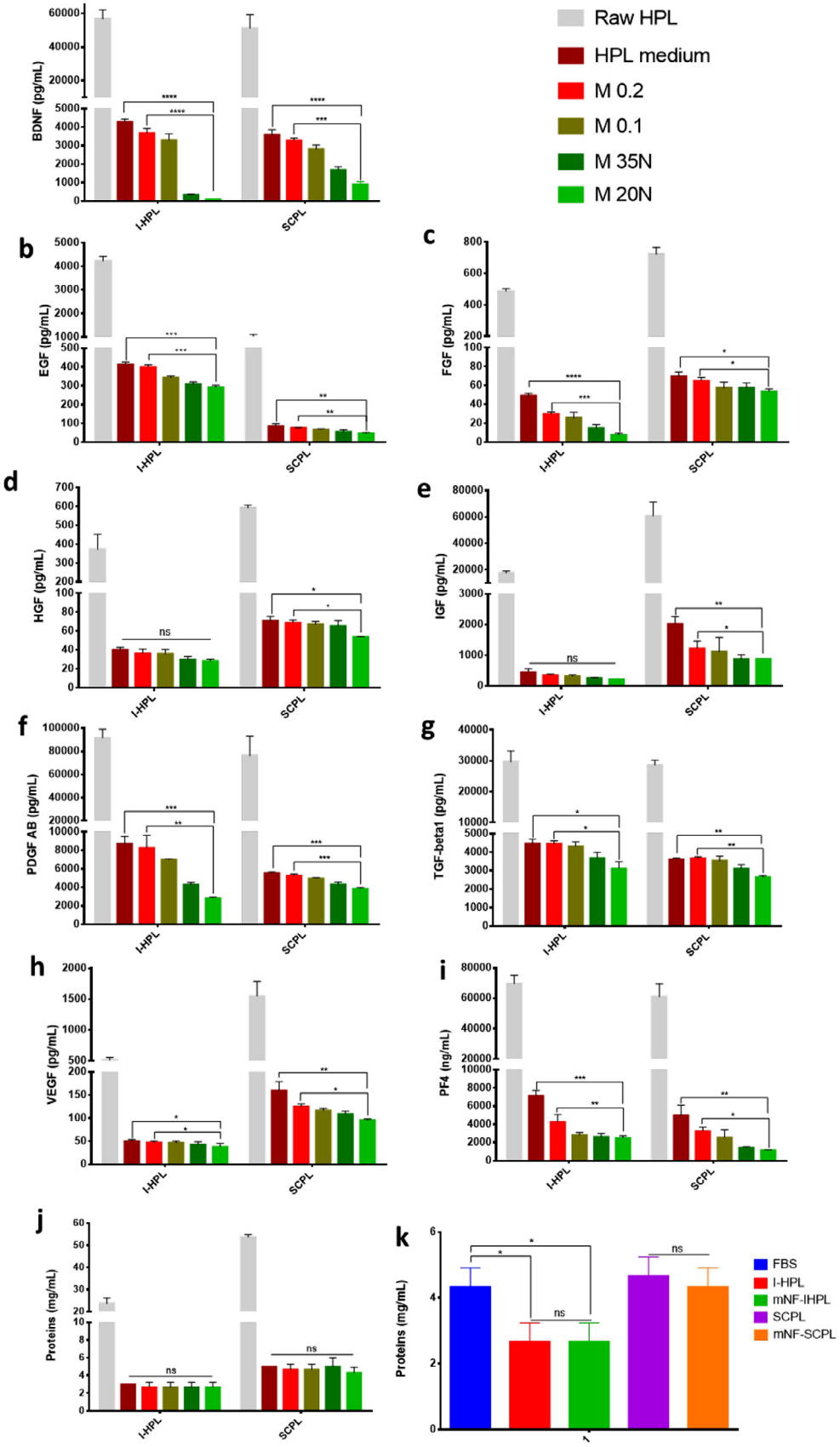

Figure 2. Medium characterization; eight growth factors (A–H) and platelet factor 4 (I) analyzed by an ELISA method and total protein analyzed by BCA (J, K). Values are expressed as the mean ± SD; n = 3; * $P < 0.05$; ** $P < 0.01$; *** $P < 0.001$; **** $P < 0.0001$; ns, no significant difference. (Color version of figure is available online).

Table 4
Extracellular vesicles analysis.

I-HPL	10% HPL in DMEM		0.2-μm filtration		0.1-μm filtration		35N nanofiltration		20N nanofiltration	
	Value	SD	Value	SD	Value	SD	Value	SD	Value	SD
Size (nm)	76	6.93	73.4	2.55	72.9	5.37	16.92	1.96	13.16	1.22
Concentration PEVs/mL	5.12×10^{11}	1.48×10^{11}	4.65×10^{11}	1.68×10^{11}	4.4×10^{11}	1.6×10^{11}	1.51×10^{9} **/##	4.26×10^{8}	4.79×10^{8} **/##	1.73×10^{8}
SCPL	10% HPL in DMEM		0.2-μm filtration		0.1-μm filtration		35N nanofiltration		20N nanofiltration	
	Value	SD	Value	SD	Value	SD	Value	SD	Value	SD
Size (nm)	71.7	3.68	69.15	2.68	68.95	3.18	19.71	3.7	11.92	1.15
Concentration PEVs/mL	$9.17\ 10^{11}$	$7.21\ 10^{10}$	$8.89\ 10^{11}$	$3.37\ 10^{11}$	$3.65\ 10^{11}$*	$2.41\ 10^{11}$	$1.83\ 10^{10}$*** /+	$2.82\ 10^{9}$	$1.15\ 10^{9}$*** /+	$1.61\ 10^{8}$
EVs / BM-MSCs culture medium	FBS		I-HPL		mNF-IHPL		SCPL		mNF-SCPL	
	Value	SD	Value	SD	Value	SD	Value	SD	Value	SD
Size (nm)	85.5	0.42	85.2	0.57	92.65	3.46	61.75	0.7	76.45	2.33
Concentration EVs/mL	1.62×10^{10}	1.2×10^{10}	10.03×10^{10}	7.03×10^{10}	4.7×10^{9} #	3.5×10^{9}	4.62×10^{10}	0.2×10^{10}	1.71×10^{10}	2.7×10^{10}

*FBS or 10% HPL in DMEM vs. HPL filtered; #I-HPL vs. mNF-IHPL; +SCPL vs. mNF-SCPL. *, # or + $P < 0.05$; **, ##, or ++ $P < 0.01$; ***, ### or +++ $P < 0.001$; ****, #### or ++++ $P < 0.0001$.

Genes expression profiling during BM-MSC differentiation

Expressions of ADIPOQ and PPARG (adipogenesis) as quantified by a qPCR at days 7, 10 and 14 were lower ($P < 0.0001$) in all media supplemented with platelet lysates compared with those supplemented with FBS (Figure 6Q,R). No significant difference was observed in ADIPOQ expression among cells expanded in platelet lysate-supplemented media. However, a significant difference was found in PPARG expression ($P < 0.001$) when comparing I-HPL- and mNF-IHPL-supplemented media. In general, multiples of expression of both genes increased from days 7 to 10. The expression had decreased at day 14 compared with day 10. Expressions of RUNX2 and SOX9 (chondrogenesis) increased from days 7 to 14 and had decreased by day 21 (Figure 6T,U). Multiples of expression of RUNX2 were significantly higher ($P < 0.01$) when using mNF-IHPL compared to other supplements, followed by mNF-SCPL ($P < 0.05$) at day 7. RUNX2 was more highly expressed in human platelet lysates media than in FBS. From days 7 to 14, multiples of expression of SOX9 were significantly higher in I-HPL- ($P < 0.0001$) and SCPL-supplemented media ($P < 0.001$) than in FBS-supplemented media. *RUNX2* and *SPP1* genes expression (osteogenesis) showed significant ($P < 0.0001$) increases at day 14 with the platelet lysate media compared to FBS (Figure 6W, X). Low expressions of both genes were observed when cells were in FBS-supplemented medium.

EVs produced from BM-MSC culture

We then examined the release of EVs by BM-MSCs cultured for 72 h in media that was nanofiltered or not (Table 4, Figure 7). The NTA analysis did not show a significant difference in EV concentrations in FBS-based conditioned medium compared with conditioned media supplemented by human platelet lysates.

Impacts of nanofiltration on BM-MSC immunomodulatory properties

Results of the assessment of BM-MSCs immunosuppressive activities are shown in Figure 8. BM-MSC viability in coculture was similar under all culture conditions (Figure 8A), apart from mNF-IHPL medium where the viability was lower compared with I-HPL ($P < 0.01$). PBMC proliferation under 2% PHA activation was similar in all supplements, except when using SCPL supplementation, for which cells had higher viability than when using FBS ($P < 0.0001$). Differences were observed in PBMCs cultured with medium from BM-MSC culture ($P < 0.01$for FBS vs. I-HPL, and $P < 0.001$ for FBS vs. mNF-IHPL). The inhibition ratio of BM-MSC proliferation in co-culture (Figure 8C) was significantly higher in media supplemented with FBS compared to I-HPL ($P < 0.05$) and mNF-IHPL ($P < 0.01$). The IL-6 concentration was higher in all cocultures compared with BM-MSCs alone or to activated PBMCs. However, secretion was higher in mNF-IHPL ($P < 0.0001$) and mNF-SCPL ($P < 0.0001$) compared with FBS. IL-10 secretion was similar in all media supplements when PBMCs were activated by PHA (Figure 8e). The secretion level of TNF was very high in the PBMC/PHA culture condition, with particularly high levels in mNF-IHPL and mNF-SCPL media compared with FBS ($P < 0.0001$), I-HPL ($P < 0.0001$), and SCPL ($P < 0.0001$) media. There was less TNF in coculture conditions and when PBMCs were cultured in BM-MSC culture medium. However, lower TNF secretion was found in cocultures and PBMC culture in BM-MSC medium.

Impacts of nanofiltration on BM-MSC aging

Cell morphologies from P8 to P10 are shown in Figure 9A–O. There were significantly ($P < 0.0001$) more senescent cells in FBS-supplemented cultures than others as shown by the ratio of senescence-associated β-galactosidase (SA-β-gal)-positive cells (Figure 9Q). This ratio was higher in mNF-IHPL compared with

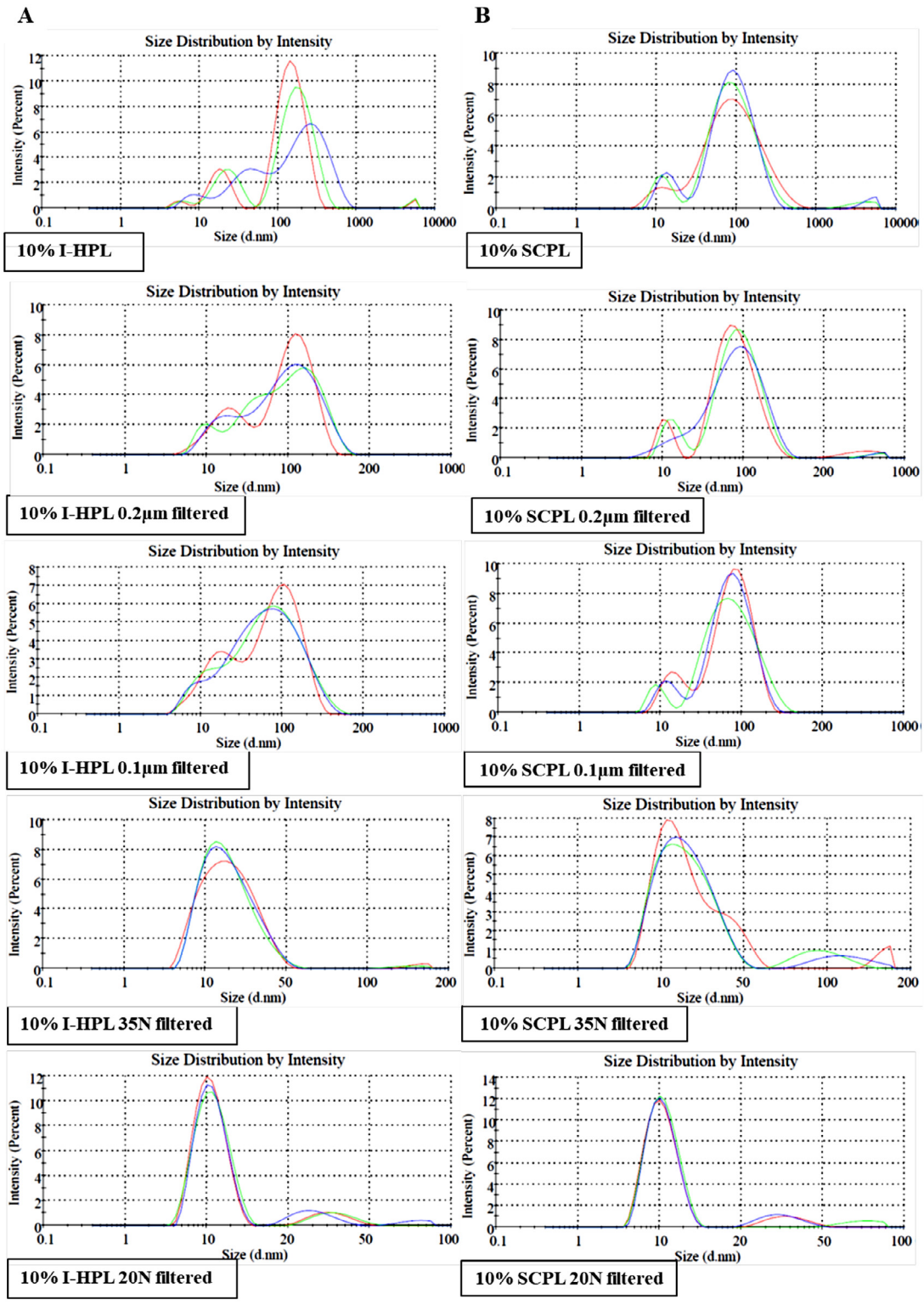

Figure 3. PEV size determination. (A) PEV size measurement by DLS in different steps of the I-HPL medium preparation process. (B) PEV size measurement by DLS in different steps of the SCPL medium preparation process. The red, green and blue curves represent the first, second, and third analyses, respectively. (Color version of figure is available online).

I-HPL ($P < 0.0001$) and in mNF-SCPL compared with SCPL ($P < 0.0001$).

Discussion

The possibility of using platelet lysate supplements in place of FBS provides a valuable xeno-free option for propagating human cells used for cell therapy procedures [2–5,10]. Pooling of a minimum number of allogeneic PC donations, needed to ensure platelet lysate consistency in quality and performance [5,27,28], increases viral risks [5,19,29]. Lysates can now be prepared from PC donations that have been pathogen-reduced by psoralen/UVA [30,31] or UV [32] treatments, without detrimentally affecting the MSC expansion capacity compared with FBS, thereby providing an important step forward in

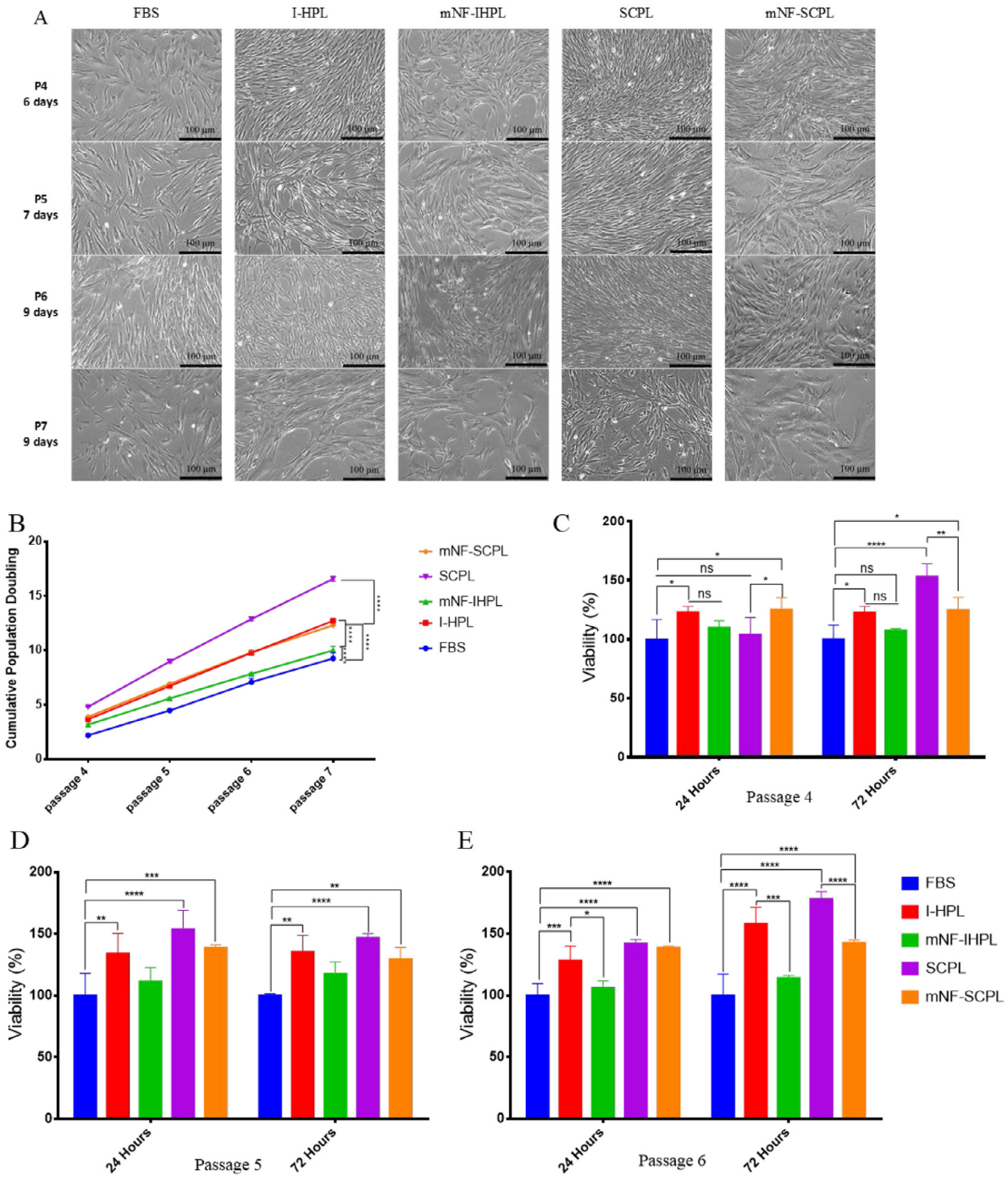

Figure 4. BM-MSC proliferation. (A) Cell morphology in different medium supplement conditions from passages 4 to 7 with culture duration per passage. (B) Cumulative population doubling from passages 4 to 7. (C, D, and E) Respectively, cell viability at passages 4, 5 and 6 in 24- and 72-h culture conditions. Viability was assessed using the CCK-8 reagent, and the Optic density (absorbance) (OD) was measured by an ELISA reader at a 450-nm wavelength. FBS culture used as the standard was set to 100%. Values are expressed as the mean ± SD; n = 3. * $P < 0.05$; ** $P < 0.01$; *** $P < 0.001$, **** $P < 0.0001$; ns, no significant difference. (Color version of figure is available online).

virus safety. Application of pathogen reduction by psoralen/UVA treatment after platelet lysis [33], and gamma-irradiation of pooled HPL [19] may also be alternative feasible approaches recently evaluated. However, all pathogen-reduction technologies have limits in their capacities, and pooling increases the risk of contamination by (i) window period donations, (ii) viruses that are not tested for, (iii) emerging infectious agents and (iv) potentially prions [13–17,19]. These reasons make the implementation of "orthogonal" pathogen-reduction treatments of platelet lysates, as done for a long time in the plasma fractionation industry [34,35], highly desirable as stressed in recent publications [5,19,29]. We recently showed the feasibility of preparing platelet lysates subjected to psoralen/UVA and solvent/detergent [22], a treatment that is highly efficient against lipid-enveloped viruses [34–36]. However, combining these two treatments may not eliminate the risk of transmission of non-enveloped viruses [37,38], such as hepatitis A virus, hepatitis E virus and parvovirus B19, justifying exploration for other pathogen-reduction procedures. Nanofiltration is recognized as being a very robust process for removing by a size-exclusion mechanism over 4 log levels of viruses that are larger than the pore-size of the membrane used. Due to its reliability and robustness, nanofiltration is widely used in the plasma fractionation and biotech industries to ensure the safety of licensed

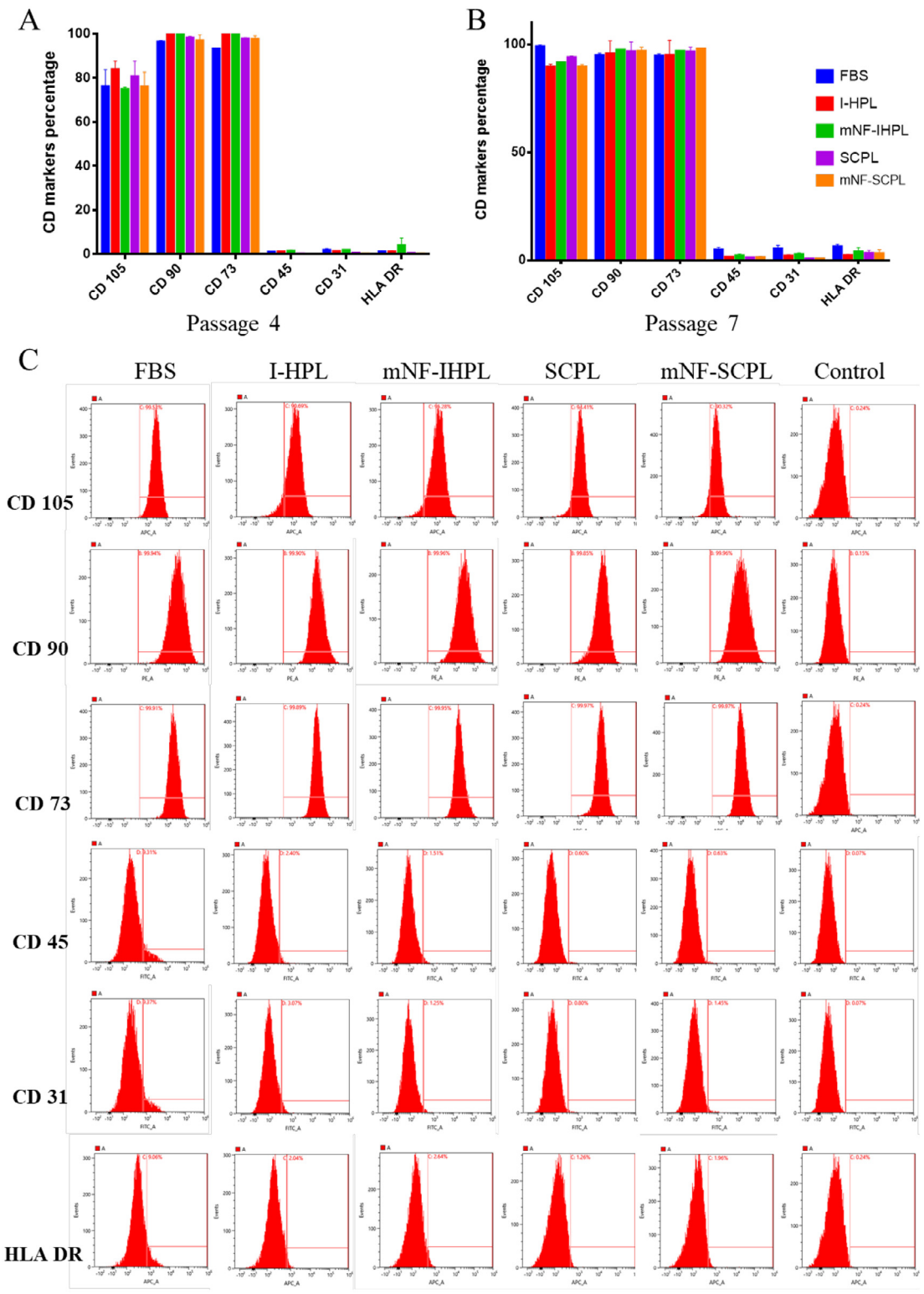

Figure 5. BM-MSC immunophenotyping. (A) Cluster of differentiation (CD) marker percentages at passage 4, the first passage in different experimental medium. (B) CD marker percentages at passage 7. (C) Flow cytometric Sony SA3800 data for different markers in different medium supplements. The control was unstained cells cultured in medium supplemented with FBS. CD105, CD90 and CD73 are positive markers; CD45, CD31 and HLA-DR are negatives markers. (Color version of figure is available online).

biologicals made from mammalian sources against pathogens [20,21,39]. Virus removal achieved by both the 35- and 20-nm nanofilters has been shown to be robust including for known small viruses such as parvovirus B19 using a wide range of filtration conditions [20,39–41]. Nanofiltration on small-pore-size filters of ≤35 nm was also found in experimental models to be effective at removing several log levels of prions [42,43]. It was therefore relevant to assess whether nanofiltration can be considered a means to improve HPL virus safety.

The main purpose of this study was therefore to determine whether nanofiltration can be considered by manufacturers to improve the pathogen safety of pooled allogeneic human platelet

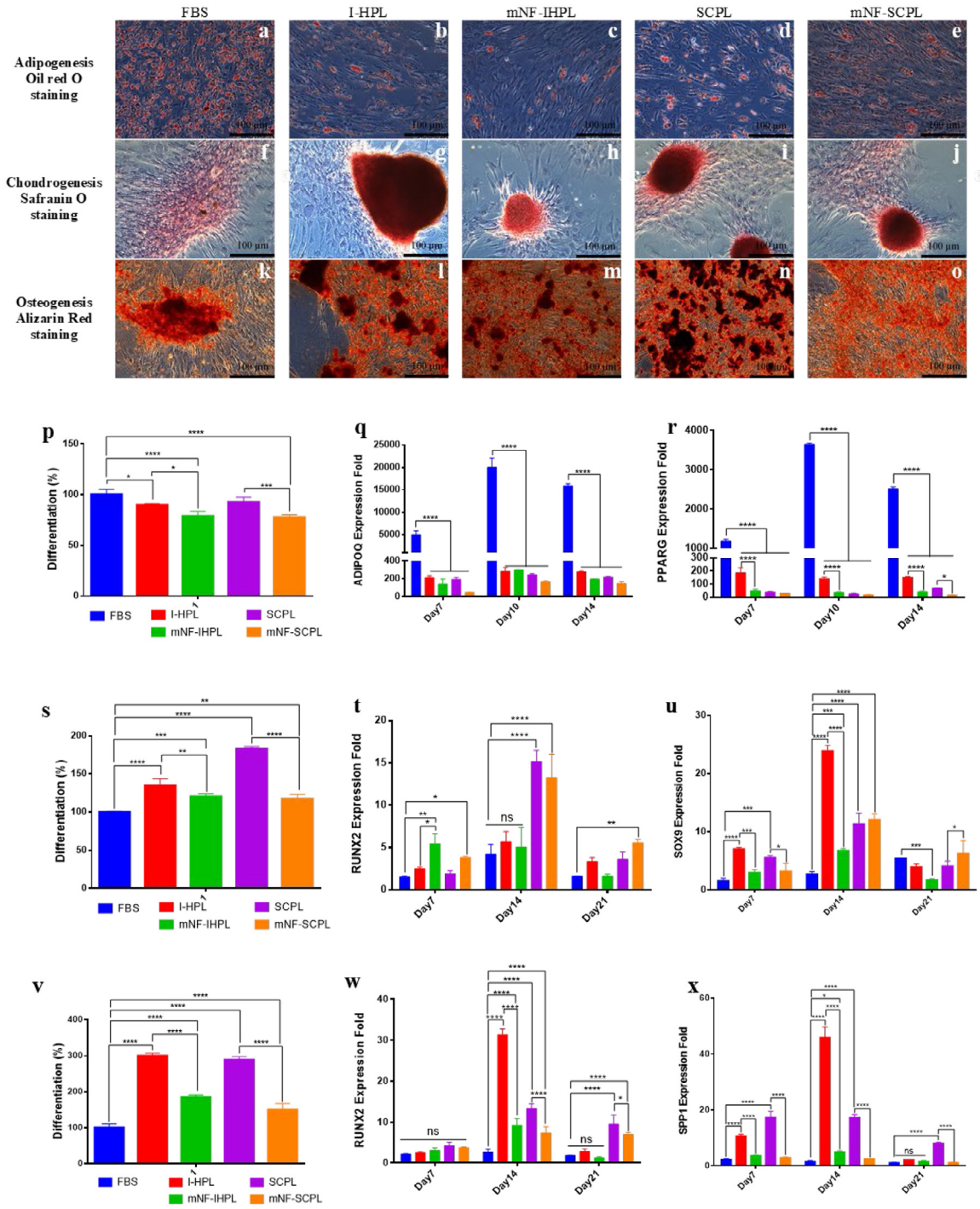

Figure 6. BM-MSC trilineage differentiation assessment: adipogenesis in different experimental media stained at 14 days with Oil Red O for lipid droplet formation evaluation (A–E); chondrogenesis stained at 21 days with Safranin O for glycosaminoglycan formation assessment (F–J); and osteogenesis stained at 21 days with Alizarin Red for calcium deposition assessment (K–O). (P) Adipogenesis quantification, (Q) *ADIPOQ* gene expression analysis at days 7, 10 and 14 of adipogenesis differentiation. (R) *PPARG* gene expression analysis at days 7, 10 and 14 of adipogenesis differentiation. (S) Glycosaminoglycan quantitative evaluation. (T) *RUNX2* gene expression analysis at days 7, 14 and 21 of chondrogenesis differentiation. (U) *SOX9* gene expression analysis at days 7, 14 and 21 of chondrogenesis differentiation. (V) Calcium deposition quantitative assessment; osteogenesis gene expression analysis at days 7, 14 and 21 for RUNX2 (w) and SPP1 (X). Values are expressed as the mean ± SD; n = 3. * $P < 0.05$; ** $P < 0.01$; *** $P < 0.001$; **** $P < 0.0001$. ns, no significant difference. (Color version of figure is available online).

lysates used as growth medium supplements for MSC expansion *in vitro*. To answer this question, we used two types of platelet lysates that are representative of those currently used by the cell therapy industry [10]. One was prepared from non–pathogen-reduced PCs suspended in 100% plasma. Platelet lysates from this source material were serum-converted by calcium chloride activation, as described by others before [1], to remove fibrinogen and avoid the need for heparin addition during cell culture [10]. Removal of fibrinogen and other high-molecular-mass coagulation factors during fibrin formation from this lysate made from PCs in 100% plasma can also facilitate the nanofiltration process because fibrinogen solutions are known to be difficult to nanofilter on 20-nm membranes [44]. The other platelet lysate was produced from PCs subjected to psoralen/UVA pathogen reduction, and suspended in a 65% SSP+ additive solution and

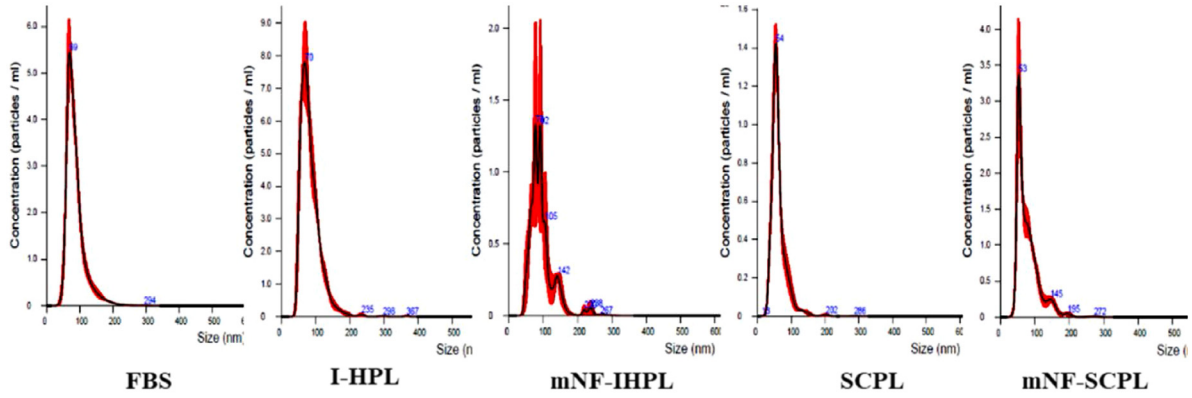

Figure 7. Extracellular vehicle (EV) size determination by a nanoparticle tracking analysis (NTA) in BM-MSC culture media after 72 h of culture. (Color version of figure is available online).

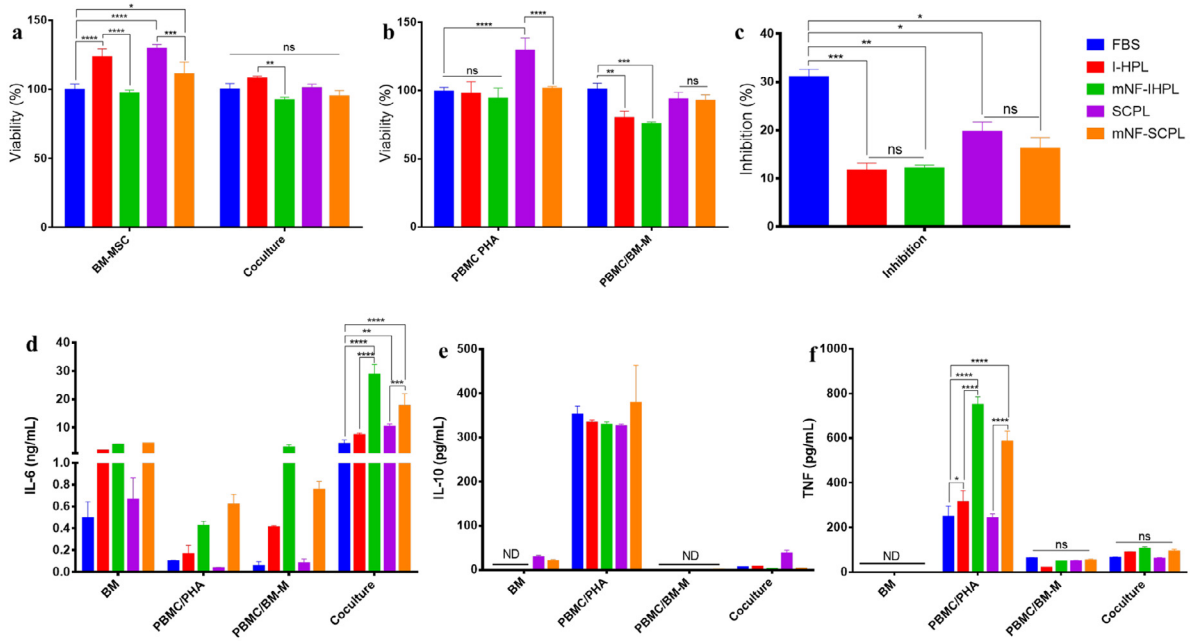

Figure 8. BM-MSC immunosuppressive activities: (A) BM-MCS 72-h culture viability at passage 8 and BM-MSCs mixed with peripheral blood mononuclear cell (PBMC) (coculture) viability. (B) PBMC culture viability assessment for 72-h culture (PBMC phytohemagglutinin (PHA): PBMC culture in RPMI1640 supplemented with 2% PHA, PBMC RPMI1640/medium from BM-MSC (BM-M): PBMC cultured in mixed medium (72 h of culture); FBS OD was used as the reference and represented 100% of viability. (C) inhibitory effects of PBMCs on BM-MSC proliferation in coculture. (D) IL-6 measurement by an ELISA method from different experimental culture media (BM: BM-MSC culture media; PBMC PHA culture media; PBMC BM-M co-culture culture media). (E) IL-10 measurement by an ELISA. (F) TNF measurement by ELISA. ND, not detectable. Values are expressed as the mean ± SD; $n = 3$. * $P < 0.05$; ** $P < 0.01$; *** $P < 0.001$; **** $P < 0.0001$; ns, no significant difference. (Color version of figure is available online).

35% plasma. This lysate was not serum-converted, as we speculated that the partial removal of plasma, resulting in a major decrease in the total protein content, could facilitate the nanofiltration process. Both HPLs were prepared from outdated PCs collected by apheresis due to availability of this material for our study. However, it has been shown that PCs prepared from buffy coats isolated from whole blood donations are equally effective as source material to prepare HPL for human cell propagation [5,10]. Nanofiltration was directly carried out on growth medium supplemented with 10% of these two platelet lysates. Medium nanofiltration was selected because (a) filtering the raw platelet lysates could result in nanofilter clogging and (b) it eliminates risks of contaminating cell cultures by adventitious pathogens that could originate from operators or raw materials [45], as evidenced by the commercial availability of dedicated medium filters that became commercially available after viral contamination of recombinant proteins took place due to GMP failures [46,47].

We found that nanofiltration largely preserved the total protein and biochemical compositions of the growth media supplemented with these two types of platelet lysates. The reasons for the decreases in the contents of BDNF, PDGF-AB and PF4 due to the nanofiltration process were unclear considering their low molecular masses but could have been due to nonspecific adsorption onto the nanofilters, as was observed before with hydrophobic chromatographic media [48]. However, the overall concentrations of growth factors evaluated remained within the expected range of platelet lysate-supplemented media [3,10,49]. A DLS analysis of the nanofiltered media showed the disappearance of the main PEV population of approximately 70 nm. The possibility of preparing PEV-depleted media for MSC culture is of interest because this avoids or decreases the risks of contaminating MSC-EVs used for clinical applications by EVs originating from growth medium supplements like FBS or platelet lysates [50–52]. Two main methods of EV depletion have been reported so far: high-speed ultracentrifugation and chemical precipitation [53,54]. Our data suggest that nanofiltration on 20-nm nanofilters may represent a powerful alternative approach for EV removal from growth media, although further evaluation remains needed to establish the robustness of such removal.

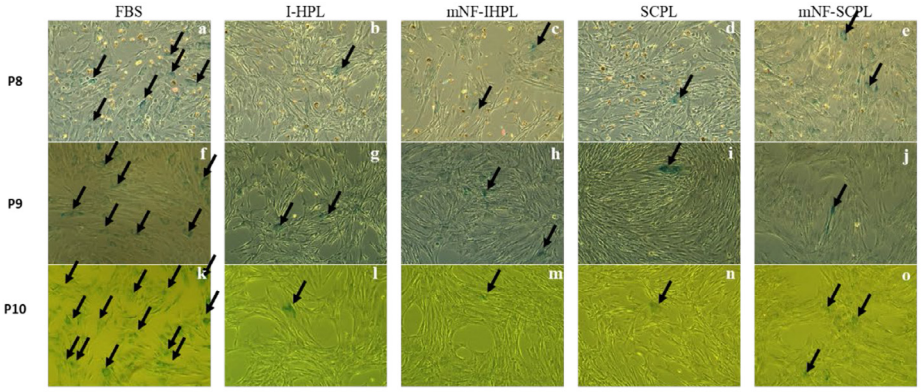

p

Passage number	Times	FBS		I-HPL		mNF-IHPL		SCPL		mNF-SCPL	
		Cells nb.	Senes. cells	Cells nb.	Senes. cells	Cells nb.	Senes. cells	Cells nb.	Senes. cells	Cells nb.	Senes. cells
Passage 8	1	205000	**29/1016**	352500	**11/1277**	197500	**15/1057**	635000	**7/1611**	252000	**13/1188**
	2	217500	**34/1237**	342000	**10/1201**	205000	**16/1135**	627000	**8/1578**	267500	**12/1209**
	3	215000	**27/977**	347000	**14/1325**	195000	**15/1048**	615000	**5/1598**	265000	**10/1075**
Passage 9	1	175000	**78/1438**	322500	**33/2020**	175000	**27/1533**	562500	**10/2498**	200000	**60/1678**
	2	180000	**75/1385**	332500	**28/1912**	202500	**26/1496**	565000	**11/2427**	187500	**65/1712**
	3	187500	**80/1583**	315000	**35/2147**	182500	**30/1621**	592500	**10/2530**	195000	**59/1567**
Passage 10	1	135000	**142/1778**	272500	**24/1893**	202500	**65/1830**	472500	**8/2376**	202500	**90/1662**
	2	142500	**138/1689**	285000	**31/2042**	190000	**68/1925**	465000	**9/2237**	197500	**87/1514**
	3	130000	**131/1802**	270000	**27/1963**	205000	**64/1791**	487500	**11/2458**	185000	**85/1487**

q

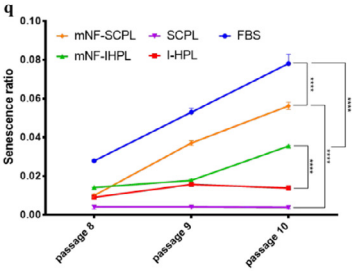

Figure 9. Senescence assay: BM-MSC senescent cell staining by X-Gal reagent at passages 8 (A–E), 9 (F–J) and 10 (K–O). (P) cell counting: cells nb., cell numbers after trypsinization, harvested cells were counted and seeded for the next passage. Senes. cells, senescent cells counted in 10 microscopic fields and total numbers of cells in the same 10 microscopy fields. (Q) senescence ratio obtained from cell counting. Arrow indicating senescent cell; values are expressed as the mean ± SD; $n = 3$. * $P < 0.05$; ** $P < 0.01$; *** $P < 0.001$; **** $P < 0.0001$; ns, no significant difference. (Color version of figure is available online).

The BM-MSCs expanded in nanofiltered platelet lysate media were better than those in FBS-supplemented media, and they maintained their stem cell phenotype, fulfilling International Society for Cell & Gene Therapy criteria [55]. CD31, a platelet–endothelial cell marker, was found negative, thereby demonstrating that the use of human platelet did not modify the lack of expression of this marker in BM-MSCs [56,57]. Over long-term culture (P8–P10), BM-MSCs expanded in nanofiltered media had an increasing ratio of senescent cells, possibly consistent with the removal of PEVs, as suggested by other studies [54,58]. Nevertheless, this ratio was still less than that found in cells expanded in FBS supplements.

BM-MSCs expanded in all platelet lysate-supplemented media could well differentiate into three lineages. The adipogenic differentiation capacity was less than that of FBS-expanded cells, as indicated by expressions of the *ADIPOQ* and *PPARG* genes that are critical for this differentiation [59]. Chondrogenesis differentiation was more effective in media supplemented with platelet lysates, as shown by the expressions of RUNX2 and SOX9, which are associated with cartilage formation. Genes expression profiles were consistent with previous studies showing up-regulation during the ECM formation phase, thereafter followed by down-regulation during the ECM maturation phase [22,60].

Up-regulation of the *RUNX2* and *SPP1* genes, which was more pronounced in all platelet lysate-expanded cells, reflects the successful capacity of BM-MSCs to differentiate into osteocytes. The relatively lower expression in nanofiltered growth media could possibly be linked in part to a decrease of FGF content because this growth factor plays a key role in osteogenesis by activating RUNX2, which regulates bone formation and growth, and participates in the anabolic function of osteoblasts [61,62]. Gene expression data obtained here are consistent with previous reports on the stronger stimulation of chondrogenic and osteogenic differentiation using human platelet lysates than FBS [22,30,63].

Data showed inhibition of TNF and IL-10 secretions, as well as suppression of PBMC proliferation in coculture conditions. Moreover, a similar immunosuppressive effect was found in PBMCs cultured in medium recovered from BM-MSC culture. Our immunosuppression data of BM-MSCs were similar to previous studies [22,64], which identified that TNF induces suppression of PBMC proliferation by triggering an MSC-mediated immunoregulatory function [65]. TNF activates transcription factors to produce IL-6 [66] as shown in coculture.

It should be kept in mind that PEV depletion, as obtained by nanofiltration, may have detrimental effects on *in vitro* cell growth, as well as viability and immunosuppressive effects [53,54,58,67]. BM-MSCs expanded in the two nanofiltered media exhibited lower proliferation rates, less viability, and higher ratios of senescent cells compared with their non-nanofiltered counterparts, possibly due to the removal of PEVs. Nevertheless, the performance of BM-MSC expansion of nanofiltered media was still superior to that of the FBS-based medium. Interestingly, concentrations of EVs released by BM-MSCs were found to be similar in all conditions, regardless of whether the medium was depleted of PEVs by nanofiltration, suggesting that using a PEV-depleted medium does not decrease or interfere with the release of EVs by MSCs. This can be of interest when MSC are used to produce EVs for therapeutic use [51,52].

Implementing a nanofiltration process has obvious advantages for optimal pathogen safety of HPL-supplemented growth media against blood-borne, as well as adventitious, viruses. Pathogen reduction of cell culture media prevents virus contaminations resulting from potential failures in the safety of raw materials and in good manufacturing practices, as has been seen in the biotech industry [68,69]. Technical options for the prevention of contamination of growth media include high-temperature short-time treatment and ultraviolet-C irradiation [70] or virus-filtration processes [71,72]. Conversely, nanofiltration of HPL-growth media implies specific measures at production scale including the creation of a dedicated virus-free area and specific working procedures intended to avoid the risks of downstream contaminations, as in the case, for instance, in the plasma fractionation industry. Finally, scalability and cost of the nanofiltration process are other factors to consider. Under our experimental conditions, we could nanofilter approximately 400 mL

of media on 0.01m^2 nanofilters, implying that 40 L of media could be nanofiltered using commercially available 1-m^2 nanofilters within 8 to 10 h. Advantages of nanofiltration over S/D treatment include (i) relative simplicity of the filtration process, (ii) no requirements to remove toxic chemicals and (iii) removal of nonlipid enveloped viruses and, possibly, prions [42,43].

One limitation of our study is the lack of virus removal experiments to demonstrate the actual clearance factor of viruses achieved with the nanofiltration sequence used. Such studies should indeed be performed by HPL-media suppliers or users, following existing guidelines, once exact manufacturing conditions are defined. However, there is ample information in the literature to support the robustness of nanofiltration at removing viruses and other pathogenic agents larger that the membrane pore size [20,21,39]. In particular, nanofiltration of plasma protein products using filters with a pore size of 35 or 19 nm provides a robust removal of emerging bloodborne viruses. For instance, clearance factor of over 4 log 10 of West Nile, Dengue and Zika viruses and model viruses with a size of approximately 40–50 nm, can readily be achieved when filtering various protein solutions on 35- or 19-nm filters identical to those used in this study [39,73]. Consistent removal of smaller viruses, like hepatitis A virus (27 nm), human parvovirus B19 (23–28 nm), or human poliovirus-1 (30 nm), has also been found using the 19-nm nanofilter [21,40,74]. An extensive data collection from the Plasma Protein Therapeutic Association, reflecting 20 years of experience in the manufacture of human plasma–derived proteins, "substantiates the effectiveness and robustness of nanofiltration in virus removal" Roth NJ, et al submitted for publication. The current SARS-CoV-2 pandemic illustrates the theoretical risk of virus contamination of ancillary material essential to cell therapy procedures. It is therefore critical to implement robust in-process virus reduction procedures capable of counterbalancing efficiently the virus risks associated with the source material or arising from possible airborne contamination. Coronaviruses, which have a size of close to 80–120 nm, should be readily removed by nanofilters with a pore size of 35 or 19 nm if present in the cell culture medium.

In conclusion, although the performance of the HPL was partially affected by nanofiltration, our data support the technical feasibility of applying a dedicated pathogen-removal nanofiltration step of growth media supplemented with two standard human platelet lysates. In particular, nanofiltration can be applied to lysates derived from pathogen-reduced PCs, making the end-product for cell expansion subjected to two complementary reduction treatments. The robustness of such nanofiltration process to remove viruses and prions should be validated by HPL users on a case-by-case basis using relevant experimental models and following guidelines. The possibility of implementing nanofiltration and double pathogen-reduction steps may turn out to offer a favorable cost–benefit ratio for the future industrial development of pooled HPLS as safe supplements for the *ex vivo* propagation of MSC-based medicinal products.

Funding

This study was partially funded by Asahi Kasei Medical (Tokyo, Japan) through a research collaboration agreement with Taipei Medical University. The sponsor played no role in data collection, analysis, or interpretation, manuscript writing or the decision to submit the article for publication.

Declaration of Competing Interest

NW and MT are employees of Asahi Kasei Medical. The other authors have no commercial, proprietary or financial interest in the products or companies described in this article.

Author Contributions

Initial conception of the study: TB, NW and MT. Design and approval of the study: LB, ON, MSC, YWW, MBCK, FK, NB, MT and TB. Supply of material: FK, NW, MT and YWW. Supervision: FK and TB. Acquisition of data: LB. Analysis and interpretation of data: LB, NB, MT and TB; Drafting of the manuscript: LB and TB. Revision of the manuscript: LB, ON, MSC; YWW; MBCK; FK, NW, MT and TB. All authors approved the final article.

Acknowledgments

We thank the Uppsala University blood bank and Taipei Blood Center (Guandu, Taiwan) for supplying platelet concentrates. We acknowledge Professor Rita Yen-Hua Huang for providing BM-MSCs. We also thank Wilson Fang-Wei Hsiang for FCM technical support.

Supplementary materials

Supplementary material associated with this article can be found in the online version at doi:10.1016/j.jcyt.2020.04.099.

References

[1] Bieback K, Hecker A, Kocaomer A, Lannert H, Schallmoser K, Strunk D, et al. Human alternatives to fetal bovine serum for the expansion of mesenchymal stromal cells from bone marrow. Stem Cells 2009;27:2331–41.
[2] Henschler R, Gabriel C, Schallmoser K, Burnouf T, Koh MBC. Human platelet lysate current standards and future developments. Transfusion 2019;59:1407–13.
[3] Shih DT-B, Burnouf T. Preparation, quality criteria, and properties of human blood platelet lysate supplements for ex vivo stem cell expansion. New Biotechnol 2015;32:199–211.
[4] Strunk D, Lozano M, Marks D, Loh Y, Gstraunthaler G, Schennach H, et al. International Forum on GMP–grade human platelet lysate for cell propagation: summary. Vox sanguinis 2018;113:80–7.
[5] Schallmoser K, Henschler R, Gabriel C, Koh MBC, Burnouf T. Production and quality requirements of human platelet lysate: a position statement from the working party on cellular therapies of the international society of blood transfusion. Trends Biotechnol 2020;38:13–23.
[6] Pittenger MF, Mackay AM, Beck SC, Jaiswal RK, Douglas R, Mosca JD, et al. Multilineage potential of adult human mesenchymal stem cells. Science 1999;284:143–7.
[7] Astori G, Amati E, Bambi F, Bernardi M, Chieregato K, Schafer R, et al. Platelet lysate as a substitute for animal serum for the ex-vivo expansion of mesenchymal stem/stromal cells: present and future. Stem Cell Res Ther 2016;7:93–100.
[8] Dessels C, Durandt C, Pepper MS. Comparison of human platelet lysate alternatives using expired and freshly isolated platelet concentrates for adipose-derived stromal cell expansion. Platelets 2019;30:356–67.
[9] Bieback K, Fernandez-Muñoz B, Pati S, Schäfer R. Gaps in the knowledge of human platelet lysate as a cell culture supplement for cell therapy: a joint publication from the AABB and the International Society of Cell Therapy. Cytotherapy 2019;21:911–24.
[10] Burnouf T, Strunk D, Koh MB, Schallmoser K. Human platelet lysate: replacing fetal bovine serum as a gold standard for human cell propagation. Biomaterials 2016;76:371–87.
[11] Schallmoser K, Bartmann C, Rohde E, Reinisch A, Kashofer K, Stadelmeye E, et al. Human platelet lysate can replace fetal bovine serum for clinical–scale expansion of functional mesenchymal stromal cells. Transfusion 2007;47:1436–46.
[12] Kocaoemer A, Kern S, Klüter H, Bieback K. Human AB serum and thrombin–activated platelet–rich plasma are suitable alternatives to fetal calf serum for the expansion of mesenchymal stem cells from adipose tissue. Stem cells 2007;25:1270–8.
[13] Musso D, Stramer SL, Committee AT-TD, Busch MP, International Society of Blood Transfusion Working Party on Transfusion-Transmitted Infectious D. Zika virus: a new challenge for blood transfusion. Lancet 2016;387:1993–4.
[14] Marano G, Pupella S, Vaglio S, Liumbruno GM, Grazzini G. Zika virus and the never-ending story of emerging pathogens and transfusion medicine. Blood Transfus 2016;14:95–100.
[15] Pisani G, Cristiano K, Pupella S, Liumbruno GM. West Nile virus in Europe and safety of blood transfusion. Transfus Med Hemother 2016;43:158–67.
[16] Levi JE. Dengue virus and blood transfusion. J Infect Dis 2016;213:689–90.
[17] Pan Y, Zhang D, Yang P, Poon LL, Wang Q. Viral load of SARS-CoV-2 in clinical samples. The Lancet Infect Dis 2020;20:411–2.
[18] CPMP Note for guidance on plasma -derived medicinal products. CPMP/BWP/269/95 rev.4. http://www.emea.eu.int; 2009. [accessed Jan 5, 2019].
[19] Blümel J, Schwantes A, Baylis SA, Stühler A. Strategies toward virus and prion safe human platelet lysates. Transfusion 2020;60:219–20.
[20] Burnouf T, Radosevich M. Nanofiltration of plasma–derived biopharmaceutical products. Haemophilia 2003;9:24–37.

[21] Inouye M, Burnouf T. The role of nanofiltration in the pathogen safety of biologicals: an update. Current Nanoscience 2019;15:1–10.
[22] Barro L, Su YT, Nebie O, Wu YW, Huang YH, Koh MBC, et al. A double–virally–inactivated (Intercept–solvent/detergent) human platelet lysate for in vitro expansion of human mesenchymal stromal cells. Transfusion 2019;59:2061–73.
[23] 5.2.12. Raw materials of biological origin for the production of cell-based and gene therapy medicinal products—European Pharmacopoeia eu/en/ph-eur-9th-edition. Council of Europe 2016.
[24] Chen M-S, Wang T-J, Lin H-C, Burnouf T. Four types of human platelet lysate, including one virally inactivated by solvent-detergent, can be used to propagate Wharton jelly mesenchymal stromal cells. New biotechnology 2019;49:151–60.
[25] Strandberg G, Sellberg F, Sommar P, Ronaghi M, Lubenow N, Knutson F, et al. Standardizing the freeze-thaw preparation of growth factors from platelet lysate. Transfusion 2017;57:1058–65.
[26] Himal I, Goyal U, Ta M. Evaluating Wharton's jelly–derived mesenchymal stem cell's survival, migration, and expression of wound repair markers under conditions of ischemia-like stress. Stem Cells Int 2017;2017:5259849.
[27] Schallmoser K, Strunk D. Preparation of pooled human platelet lysate (pHPL) as an efficient supplement for animal serum-free human stem cell cultures. J Vis Exp 2009. https://doi.org/10.3791/1523.
[28] Viau S, Lagrange A, Chabrand L, Lorant J, Charrier M, Rouger K, et al. A highly standardized and characterized human platelet lysate for efficient and reproducible expansion of human bone marrow mesenchymal stromal cells. Cytotherapy 2019;21:738–54.
[29] Burnouf T, Barro L, Nebie O, Wu YW, Goubran H, Knutson F, et al. Viral safety of human platelet lysate for cell therapy and regenerative medicine: moving forward, yes, but without forgetting the past. Transfus Apher Sci 2019;58:102674.
[30] Jonsdottir-Buch SM, Sigurgrimsdottir H, Lieder R, Sigurjonsson OE. Expired and pathogen-inactivated platelet concentrates support differentiation and immunomodulation of mesenchymal stromal cells in culture. Cell Transplant 2015;24:1545–54.
[31] Fazzina R, Iudicone P, Mariotti A, Fioravanti D, Procoli A, Cicchetti E, et al. Culture of human cell lines by a pathogen-inactivated human platelet lysate. Cytotechnology 2016;68:1185–95.
[32] Viau S, Chabrand L, Eap S, Lorant J, Rouger K, Goudaliez F, et al. Pathogen reduction through additive-free short-wave UV light irradiation retains the optimal efficacy of human platelet lysate for the expansion of human bone marrow mesenchymal stem cells. PLoS One 2017;12:e0181406.
[33] Christensen C, Jonsdottir-Buch SM, Sigurjonsson OE. Effects of amotosalen treatment on human platelet lysate bioactivity: a proof-of-concept study. PLoS One 2020;15:e0220163.
[34] Burnouf T, Radosevich M. Reducing the risk of infection from plasma products: specific preventative strategies. Blood Rev 2000;14:94–110.
[35] Burnouf T. Modern plasma fractionation. Transfus Med Rev 2007;21:101–17.
[36] Dichtelmuller HO, Biesert L, Fabbrizzi F, Gajardo R, Groner A, von Hoegen I, et al. Robustness of solvent/detergent treatment of plasma derivatives: a data collection from Plasma Protein Therapeutics Association member companies. Transfusion 2009;49:1931–43.
[37] Kwon SY, Kim IS, Bae JE, Kang JW, Cho YJ, Cho NS, et al. Pathogen inactivation efficacy of Mirasol PRT System and Intercept Blood System for non-leucoreduced platelet-rich plasma-derived platelets suspended in plasma. Vox Sang 2014;107:254–60.
[38] Gowland P, Fontana S, Stolz M, Andina N, Niederhauser C. Parvovirus B19 Passive transmission by transfusion of Intercept® blood system-treated platelet concentrate. Transfus Med Hemother 2016;43:198–202.
[39] Caballero S, Diez JM, Belda FJ, Otegui M, Herring S, Roth NJ, et al. Robustness of nanofiltration for increasing the viral safety margin of biological products. Biologicals 2014;42:79–85.
[40] Hongo-Hirasaki T, Yamaguchi K, Yanagida K, Okuyama K. Removal of small viruses (parvovirus) from IgG solution by virus removal filter Planova® 20N. J Membrane Sci 2006;278:3–9.
[41] Adan–Kubo J, Tsujikawa M, Takahashi K, Hongo–Hirasaki T, Sakai K. Microscopic visualization of virus removal by dedicated filters used in biopharmaceutical processing: impact of membrane structure and localization of captured virus particles. Biotechnol Prog 2019;35:e2875.
[42] Flan B, Arrabal S. Manufacture of plasma-derived products in France and measures to prevent the risk of vCJD transmission: precautionary measures and efficacy of manufacturing processes in prion removal. Transfus Clin Biol 2007;14:51–62.
[43] Burnouf T, Padilla A. Current strategies to prevent transmission of prions by human plasma derivatives. Transfus Clin Biol 2006;13:320–8.
[44] Schulz PM, Gehringer W, Nohring S, Muller S, Schmidt T, Kekeiss-Schertler S, et al. Biochemical characterization, stability, and pathogen safety of a new fibrinogen concentrate (fibryga®). Biologicals 2018;52:72–7.
[45] Kerr A, Nims R. Adventitious Viruses Detected in Biopharmaceutical Bulk Harvest Samples over a 10 Year Period. PDA J Pharm Sci Technol 2010;64:481–5.
[46] Carbrello C, Nhiem D, Priest M, Mann K, Greenhalgh P. Supplement: upstream virus safety: protect your bioreactor by media filtration. Genet Engineer Biotechnol News 2017;37 https://www.genengnews.com/category/magazine/301/.
[47] Mann K, Royce J, Carbrello C, Smith R, Zhu R, Zeng Y, et al. Protection of bioreactor culture from virus contamination by use of a virus barrier filter. BMC Proceedings 2015;9:22–4.
[48] Su CY, Kuo YP, Lin YC, Huang CT, Tseng YH, Burnouf T. A virally inactivated functional growth factor preparation from human platelet concentrates. Vox Sang 2009;97:119–28.
[49] Kao Y-C, Bailey A, Samminger B, Tanimoto J, Burnouf T. Removal process of prion and parvovirus from human platelet lysates used as clinical-grade supplement for ex vivo cell expansion. Cytotherapy 2016;18:911–24.
[50] Gomzikova M, James V, Rizvanov A. Therapeutic application of mesenchymal stem cells derived extracellular vesicles for immunomodulation. Front Immunol 2019;10:2663.
[51] Agrahari V, Agrahari V, Burnouf P-A, Chew CH, Burnouf T. Extracellular microvesicles as new industrial therapeutic Frontiers. Trends Biotechnol 2019;37:707–29.
[52] Burnouf T, Agrahari V, Agrahari V. Extracellular vesicles as nanomedicine: hopes and hurdles in clinical translation. Int J Nanomed 2019;14:8847–59.
[53] Lehrich B, Liang Y, Khosravi P, Federoff H, Fiandaca M. Fetal bovine serum-derived extracellular vesicles persist within vesicle-depleted culture media. Int J Mol Sci 2018;19:3538–49.
[54] Aswad H, Jalabert A, Rome S. Depleting extracellular vesicles from fetal bovine serum alters proliferation and differentiation of skeletal muscle cells in vitro. BMC Biotechnol 2016;16:32.
[55] Dominici M, Le Blanc K, Mueller I, Slaper-Cortenbach I, Marini F, Krause D, et al. Minimal criteria for defining multipotent mesenchymal stromal cells. The International Society for Cellular Therapy position statement. Cytotherapy 2006;8:315–7.
[56] Liu L, CD31 Shi G-P. beyond a marker for endothelial cells. Cardiovasc Res 2012;94:3–5.
[57] Conget PA, Minguell JJ. Phenotypical and functional properties of human bone marrow mesenchymal progenitor cells. J Cell Physiol 1999;181:67–73.
[58] Eitan E, Zhang S, Witwer KW, Mattson MP. Extracellular vesicle–depleted fetal bovine and human sera have reduced capacity to support cell growth. J Extracell Vesicles 2015;4:26373.
[59] Tencerova M, Kassem M. The bone marrow-derived stromal cells: commitment and regulation of adipogenesis. Front Endocrinol 2016;7. https://doi.org/10.3389/fendo.2016.00127.
[60] Nishimura R, Hata K, Matsubara T, Wakabayashi M, Yoneda T. Regulation of bone and cartilage development by network between BMP signalling and transcription factors. J Biochem 2012;151:247–54.
[61] Xiao G, Jiang D, Gopalakrishnan R, Franceschi RT. Fibroblast growth factor 2 induction of the osteocalcin gene requires MAPK activity and phosphorylation of the osteoblast transcription factor, Cbfa1/Runx2. J Biol Chem 2002;277:36181–7.
[62] Majidinia M, Sadeghpour A, Yousefi B. The roles of signaling pathways in bone repair and regeneration. J Cell Physiol 2018;233:2937–48.
[63] Zhao Z, Liu J, Weir MD, Zhang N, Zhang L, Xie X, et al. Human periodontal ligament stem cells on calcium phosphate scaffold delivering platelet lysate to enhance bone regeneration. RSC Adv 2019;9:41161–72.
[64] Boland L, Burand AJ, Brown AJ, Boyt D, Lira VA, Ankrum JA. IFN-γ and TNF-α pre-licensing protects mesenchymal stromal cells from the pro-inflammatory effects of palmitate. Mol Ther 2018;26:860–73.
[65] Dorronsoro A, Ferrin I, Salcedo JM, Jakobsson E, Fernández–Rueda J, Lang V, et al. Human mesenchymal stromal cells modulate T–cell responses through TNF–α–mediated activation of NF–κB. Eur J Immunol 2014;44:480–8.
[66] Tanaka T, Narazaki M, Kishimoto T. IL-6 in inflammation, immunity, and disease. Cold Spring Harbor Perspect Biol 2014;6:a016295.
[67] Beninson LA, Fleshner M. Exosomes in fetal bovine serum dampen primary macrophage IL-1β response to lipopolysaccharide (LPS) challenge. Immunol Lett 2015;163:187–92.
[68] Aranha H. Virus Safety of Biopharmaceuticals—absence of evidence is not evidence of absence. Contract Pharma 2011. Nov–Dec:82-7.
[69] Moody M, Alvez W, Varghese J, Khan F. Mouse minute virus (MMV) contamination—a case study: detection, root cause determination, and corrective actions. PDA J Pharm Sci Technol 2011;65:580–8.
[70] Roush JD. Integrated viral clearance strategies—reflecting on the present, projecting to the future. Curr Opin Biotechnol 2018;53:137–43.
[71] Carbrello C, Nhiem D, Priest M, Mann K, Greenhalgh P. Supplement: upstream virus safety: protect your bioreactor by media filtration. Genet Engineer Biotechnol News 2017;37.
[72] Mann K, Royce J, Carbrello C, Smith R, Zhu R, Zeng Y, et al. Protection of bioreactor culture from virus contamination by use of a virus barrier filter. BMC Proceedings 2015;9:22.
[73] Poelsler G, Berting A, Kindermann J, Spruth M, Hammerle T, Teschner W, et al. A new liquid intravenous immunoglobulin with three dedicated virus reduction steps: virus and prion reduction capacity. Vox Sang 2008;94:184–92.
[74] Caballero S, Nieto S, Gajardo R, Jorquera JI. Viral safety characteristics of Flebogamma DIF, a new pasteurized, solvent-detergent treated and Planova 20 nm nanofiltered intravenous immunoglobulin. Biologicals 2010;38:486–93.